Disc-shaped LIM for levitation and traction force control powered by the source using the component synchronous with the motor speed

TOSHIMITSU MORIZANE, KEISUKE TSURUYA, NORIYUKI KIMURA, HIDEKI OMORI

Osaka Institute of Technology
Asahi-ku, Ohimiya 5-16-1, 535-8585 Osaka, Japan
e-mail: toshimitsu.morizane@oit.ac.jp

Abstract: It has been proposed that a novel maglev transport system uses both of the attractive force and thrust force of the Linear Induction Motor (LIM). In our proposal, these two forces will be controlled by two different frequency components. One of the frequency components is synchronous with the motor speed (f_m). Another frequency component is drive frequency (f_d). Our proposed system enables the independent and simultaneous control of the attractive and thrust force of LIM. Each value of the attractive and the thrust force generated by f_m and f_d must be identified in order to design that LIM control system. For these purpose, a disc-shaped LIM has been developed as an experimental equipment. The force profiles, especially around zero slip, have been analyzed under experimental conditions.

Key words: linear induction motor, magnetically levitation, traction and levitation control, disc-shaped LIM

1. Introduction

Nowadays, LIMs are applied in the industrial factories and public transportation. The merit of LIM is that it has a simple structure and can move forward without creating dust and with minimal noise [1]. Dust displacement is especially undesirable in places such as pharmaceutical, food and semiconductor factories. LIMs are considered to be the best way of conveying some items.

In a typical system, LIMs are used as traction control devices [2-6]. Levitation magnets are used as levitation control devices [7] as shown in Figure 1. The attractive force produced by LIMs are regarded as a disturbance.

However, our proposed system will make good use of LIMs' attractive force by using a frequency component synchronous with motor speed, which means this system will not require levitation magnets [8, 9]. Moreover, this system has other advantages, being easy to maintain and reducing carrier body manufacturing costs.

This paper details a disc-shaped LIM implement in the experimental equipment and the method of measuring forces. It is necessary to convert the rotary characteristics measured with the disc-shaped LIM into the liner motion characteristics [10]. The characteristics of the attractive and the thrust force are identified in order to design that LIM control system. The attractive and thrust force are measured, especially around zero slip.
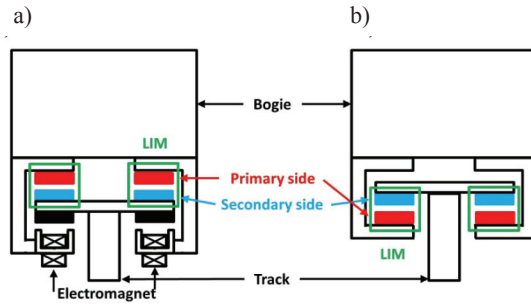

Fig. 1. Typical maglev system construction and proposed maglev system construction:
a) typical maglev system, b) proposed system

2. Design of controller for attractive force and thrust force

2.1. Proposed attractive and thrust force control

Figure 2 shows the ordinary force control using two frequency components. In this system, we have to consider the interference of two frequency components.

It is proposed that the frequency component synchronous with motor speed, f_m and the drive frequency component f_d are used as shown in Figure 3. The frequency component, f_m does not generate the thrust force, because the frequency is controlled to synchronize with the motor speed where the slip is zero. Therefore, the total thrust force can be controlled only by the frequency component, f_d. On the other hand, both frequency components generate the attractive force [11].
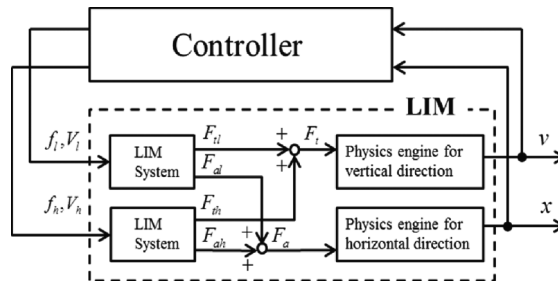

Fig. 2. Control System of the LIM using power source with two different frequency components
(F_t – total thrust force; F_a – total attractive force; f_h – higher frequency component;
V_h – Voltage of f_h; F_{th} – thrust force of fh; F_{ah} – attractive force of fh; F_l – lower frequency
component; V_l – voltage force of fl; F_{tl} – thrust force of fl; F_{al} – attractive force of fl)
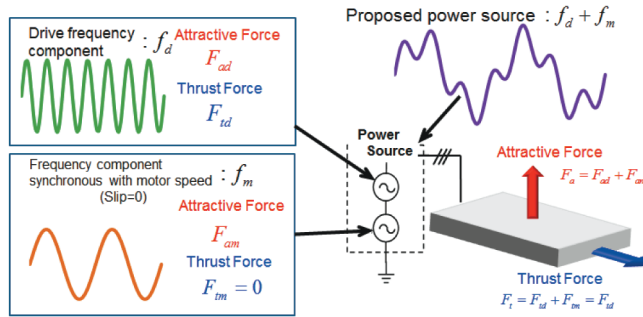
Fig. 3. Proposed attractive force and thrust force control

2.2. Proposed attractive and thrust force control

Figure 4 shows the proposed controller of the traction and levitation. When the LIM is driven by the power source consisting of the frequency components f_m and f_d, only the drive frequency component f_d generates the thrust force F_{td} for the traction because of no thrust force ($F_{tm} = 0$). Therefore the total thrust force F_t can be controlled only by the drive frequency component f_d. The frequency component f_d usually generates the attractive force F_{ad} not enough to suspend the bogie. The attractive force F_{am} generated by the frequency component f_m adjusts the total attractive force F_a. The proposed control system becomes simple since the controller for the thrust force and the attractive force are considered separately.
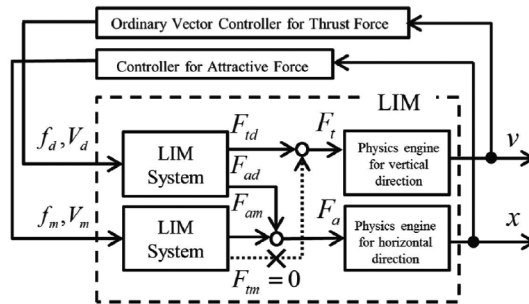

Fig. 4. Proposed control system of the LIM using power source with the frequency Component Synchronous with the Motor Speed (F_t – total thrust force; F_a – total attractive force; f_d – frequency for drive; V_d – voltage of f_d; F_{td} – thrust force of frequency f_d; F_{ad} – attractive force of f_d; f_m – frequency synchronous with mover speed; V_m – voltage of f_m; F_{tm} – thrust force of f_m; F_{am} – attractive force of f_m)

3. Experimental equipment

3.1. Experimental setup

The experimental equipment is shown in Figure 5. The disk-shaped secondary side is used to measure the drive characteristics of the LIM. The primary side is installed beneath the disc-shaped secondary side. The optical tachometer measures the revolution speed of the disk-shaped

secondary side. The assist motor is installed to assist the rotation of the LIM in order to measure forces at any slip.
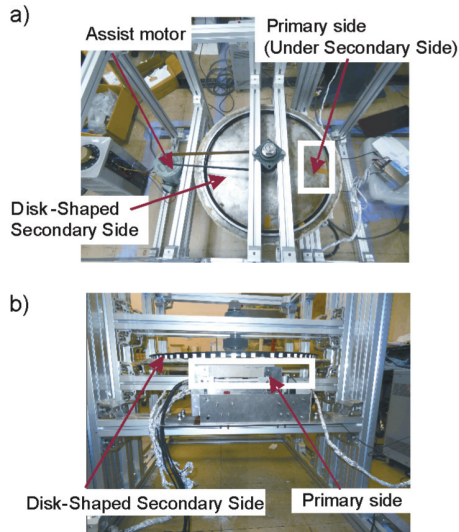

Fig. 5. Experimental Setup: a) top view, b) side view

Table 1 shows the parameters of the LIM. The primary side and load cells are shown in Figure 6. This load cell has a measurement error of 1% of 50 N.

Table 1 The parameters of the LIM

Primary side	
Size of primary side [mm]	$230(l) \times 150(w) \times 45(h)$
Weight [kg]	7.4
Pole pitch τ[mm]	45
Pole number p	4
Nominal voltage [V]	125
Nominal current [A]	125 VAC 24 VDC
	5 A 3 A
Secondary side	
Diameter [mm]	700
Thickness [mm]	Aluminum: 2.0
	Iron: 4.0

3.2. Drive system of LIM

The drive system of the LIM is shown in Figure 7. The variable autotransformer is connected with the three-phase power source, 60 Hz and 200 V. The variable autotransformer adjusts the input DC voltage of the voltage source inverter (MWINV-9R122B: Myway Corp. Yokohama)

rectified by the diode rectifier. The voltage source inverter provides the three-phase AC voltage to drive the LIM.
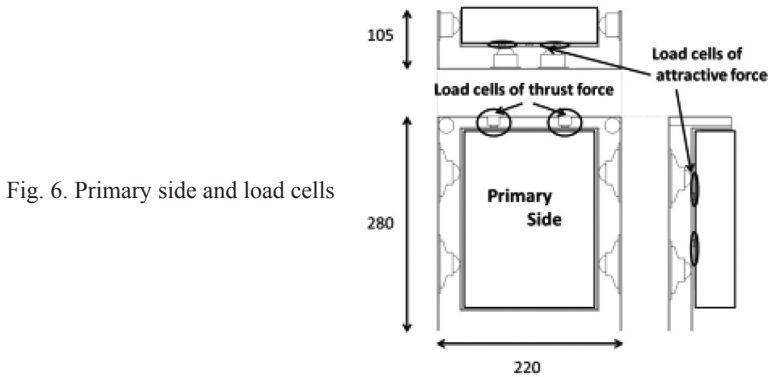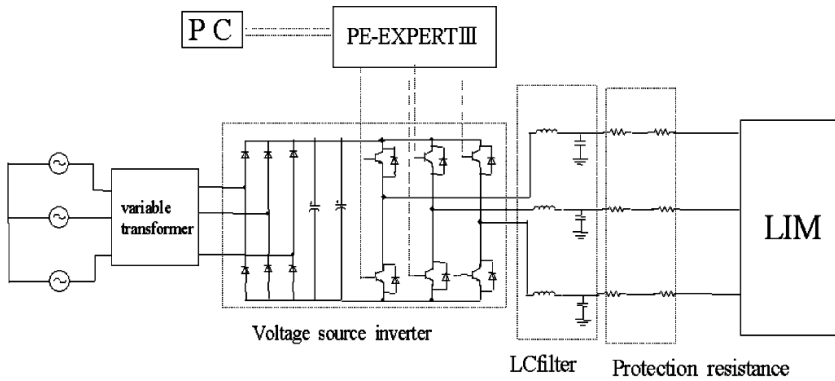

Fig. 6. Primary side and load cells

Fig. 7. LIM drive system

The voltage and frequency of the inverter is controlled by PE-EXPART III (Myway Corp. Yokohama) and DSP (TM567: Myway Corp. Yokohama). The protective resistance is connected in order to protect from the large current, when the LIM is driven with a low frequency.

4. Conversion of characteristics into linear motion

Figure 8 shows the velocity vector of the secondary side in the proposed experimental equipment [12]. The velocity of the secondary side is different by the radius of gyration. For example, velocity v' and v'' are different. As a result, the relative velocity of the secondary against the primary side is also different. It is necessary to estimate the equivalent velocity and equivalent slip in the linear motion.

Figure 9 shows the X-Y coordinate of the secondary side to estimate the equivalent velocity. The origin point, O, of the coordinate is set to the center of the rotation of a secondary side. The X-axis is defined to the direction of the traveling magnetic field generated by a primary side. The

Y-axis is set to the direction of the radius where the X-axis and Y-axis are orthogonal as shown in Figure 9. It is assumed that the disk is rotating in a clockwise direction in ω_m[rad/s].
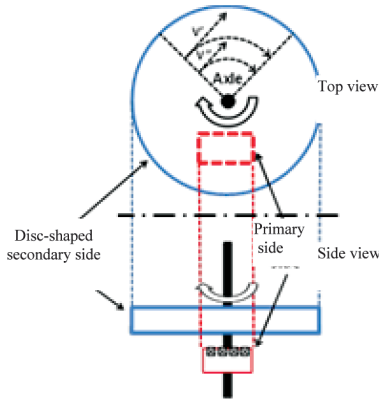

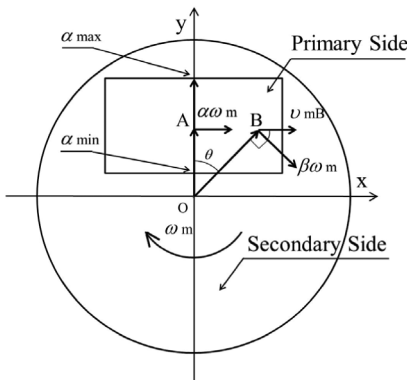Fig. 8. Experimental equipment of LIM with the disc-shaped secondary side

Fig. 9. The X-Y coordinate on the top view

Two points, point A and B are considered along the direction of the traveling magnetic field as shown in Figure 9. The coordinate of point A is $(0, \alpha)$ located on the Y axis. The distance OB between point B and the origin O is β. The angle between OA and OB is θ. The coordinate of point B is $(\beta \sin\theta, \beta \cos\theta)$ where $\beta \sin\theta = \alpha$.

The velocities of the secondary side in point A and point B have a tangential direction against the radius. The values of velocity in point A and point B are $\alpha\omega_m$, $\beta\omega_m$ respectively. The x-axis component of the velocity in point A (v_{mA}) and B (v_{mB}) are calculated in (1) respectively.

$$v_{mA} = \alpha\omega_m, \quad v_{mB} = \beta\omega_m \cos\theta = (\beta\cos\theta)\omega_m = v_{mA}. \tag{1}$$

Equation (1) indicates that the x-axis component of velocity is constant along the direction of the traveling magnetic field. It means that the *x*-axis component of the velocities against the traveling magnetic field is constant and the slip is also constant along the direction of the traveling magnetic field.

It is assumed that the primary side is located between α_{min} and α_{max} on the Y-axis, the slip $s(\alpha)$ and the average slip s_{ave} is calculated by (2).

$$s(\alpha) = \frac{2\tau f - \alpha \omega_m}{2\tau f},$$

$$s_{ave} = \frac{1}{(\alpha_{max} - \alpha_{min})}\int_{\alpha_{min}}^{\alpha_{max}} s(\alpha)d\alpha = \frac{1}{(\alpha_{max} - \alpha_{min})}\int_{\alpha_{min}}^{\alpha_{max}} \frac{2\tau f - \alpha\omega_m}{2\tau f}d\alpha \qquad (2)$$

$$= \frac{2\tau f - \frac{(\alpha_{max} + \alpha_{min})}{2}\omega_m}{2\tau f},$$

where f is frequency of the power source and τ is the pole pitch.

In the experimental equipment, the mean value of the velocity and slip represent the equivalent velocity and the equivalent slip respectively.

The effective radius (r_e), the equivalent slip of LIM (s_e) are defined as (3).

$$r_e = \frac{(\alpha_{max} + \alpha_{min})}{2}, \quad s_e = s_{ave} = \frac{2\tau f - r_e\omega_m}{2\tau f}. \qquad (3)$$

The equivalent slip frequency (f_s) is calculated by the frequency of the power source and the equivalent slip of LIM in (4) [2].

$$f_s = s_e f = \frac{2\tau f - r_e\omega_m}{2\tau}. \qquad (4)$$

5. Experimental results

The experimental measurement of the f_m's attractive and thrust force was conducted. The main purpose of this experiment was to examine the value of the attractive and thrust force generated by the f_m component at zero slip. At first we applied the voltage (31 V, 60 Hz, between V-W) to the LIM. The value of the electrical current is 3.0 A. Secondly, voltage was applied to the assist motor to help the LIM rotate faster. Then the speed of the disk-shaped secondary side was adjusted to the speed of the moving magnetic field. Finally, the number of both the attractive and thrust force around zero slip was recorded. As shown in Figure 10, the value of the attractive force generated by the f_m (3.0 A) was about 6.5 N. On the other hand, as shown in Figure 11, the value of the thrust force was about 0N. However, the measurement error of 2% of 100 N from two load cells (one load cell can measure a maximum of 50 N, and its measurement error is 1%) must be taken into account.[13] This result will be used to inform the design of the control system of the source using a component synchronous with the motor speed.
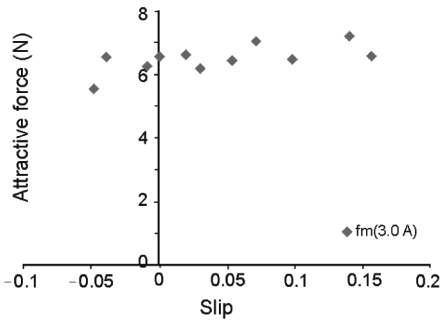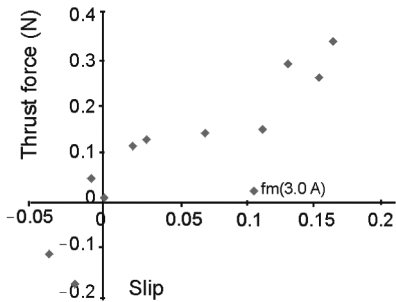
Fig. 10. Attractive force generated by f_m vs slip

Fig. 11. Thrust force generated by f_m vs slip

Table 2. Measured disc-shaped LIM parameters used in the simulation

Condition of the experimental equipment	
Thickness of the secondary side [mm]	Aluminum Iron
	0.5 4.0
Gap [mm]	Mechanical Magnetic
	4.8 5.3
The measured value of the LIM	
Primary resistance [Ω]	4.42
Primary leakage inductance [mH]	10.25
Primary self inductance [mH]	23.22
Secondary resistance [Ω]	8.80
Secondary leakage inductance [mH]	25.85
Secondary self inductance [mH]	38.82
Mutual inductance [mH]	12.97
Core-loss resistance [Ω]	0.09

6. Simulation of traction and levitation control

The control block diagram and simlation diagram using the proposed control system of LIM is shown in Figure 12 [14]. The vector controller and PI controller are applied in thrust force control, and PID controller is applied in attractive force control. Table 2 shows the measured disc-shaped LIM parameters used in the control and simulation.
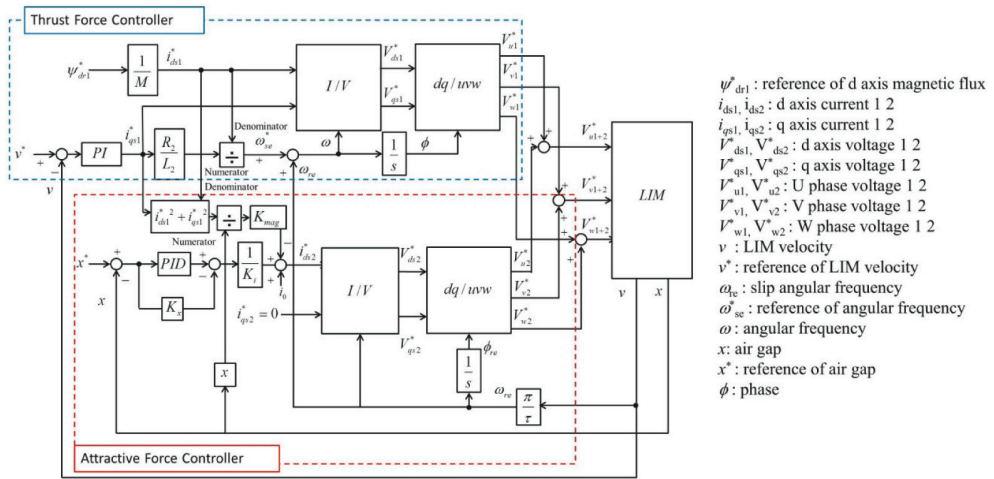
Fig. 12. Simulation of the disc-shaped LIM control using power source with frequency component synchronous with motor speed
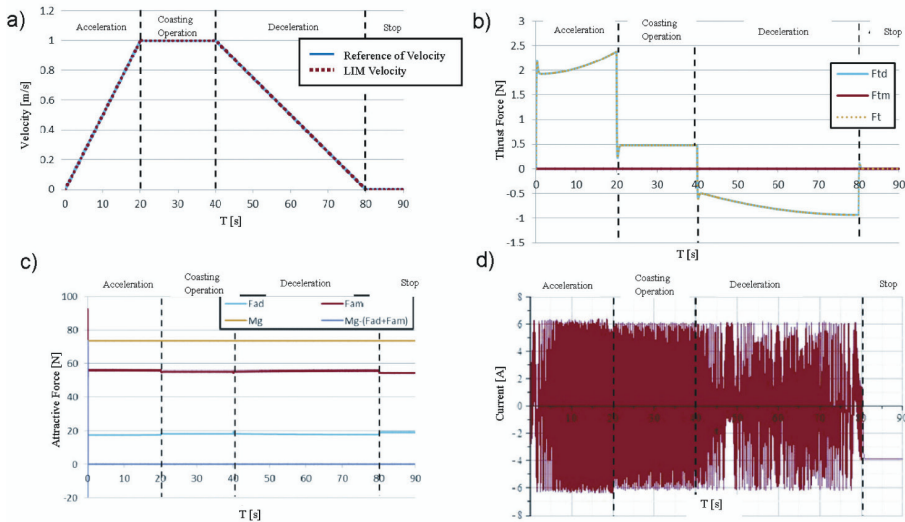

Fig. 13. Simulation results of the thrust and attractive force controller for the proposed system

Figure 13(a) shows the reference of the velocity profile of LIM and the simulation result. It has four operation modes, acceleration, coasting, deceleration, stop operation. During these mode, the total attractive force F_a ($F_{am} + F_{ad}$) is controlled to be equal to the gravity of LIM (Mg). It is clear that the velocity of LIM can be controlled according to the reference of velocity in Fig. 13 (a). As shown Figure 13(b), the total thrust force of LIM (F_t) is generated by only the drive frequency (f_d). Figure 13(c) is verified that the attractive force produced by f_d and f_m is controlled in constant in order to balance the gravity of LIM (Mg) even if the operation mode is changed. The total current (U) of $f_d + f_m$ is shown in Figure 13(d).

7. Conclusion

A novel maglev transport system is introduced. In this system, it is necessary to achieve the simultaneous and independent control of the attractive force and thrust force. These two forces will be controlled by two different frequency components. One of the frequency components is synchronous with the motor speed (f_m). Another frequency component is drive frequency (f_d). The characteristics of the attractive force and thrust force are measured with the LIM experimental equipment using the disc-shaped secondary side.

The experimental results help us to design a control system by using a component synchronous with the motor speed. The simulation results verify that the thrust and attractive force control and the velocity control of LIM is achieved simultaneously and independently by the proposed control method.

References

[1] Fujii N., Harada T., Sakamoto Y., Kayasuga T., *Compensation method for end effect of linear induction motor.* T.IEE Japan 122-D8(4): 330 (2002).

[2] Masada E., Kitano J., Mizuma T., Fujiwara S., *Trend of Linear motor car practical use.* T.IEE Japan 110-D(1): 2-7 (1990).

[3] Masada E., *Linear drive technology and application.* Ohmsha, Ltd. (1991).

[4] *Members of The Magnetic Actuator Technical Committee of The Institute of Electrical Engineers of Japan.* Linear Motor and Their Applications, Ohmsha, Ltd. (1991).

[5] Morishita M., Itoh H., The *Self-gap-detecting Zero Power Controlled Electromagnetic Suspension System.* IEEJ Trans. LA 126(12): 1667 (2006).

[6] Morishita M., Akashi M., *Guide-effective Levitation Control for Electromagnetic Suspension System.* T.IEE Japan 119-D(10): 1259 (1999).

[7] Nagano H., *Electromagnetic suspension system, HSST.* Railway Electrical engineering Association of Japan 18(7): 37-40 (2007).

[8] Morizane T., Taniguchi K., Kimura N., *Characteristics of attractive force of linear induction motor in a novel maglev system driven by the source including high frequency component.* Proc. LDIA 2003, ML-07 (2003).

[9] Takahashi I., Ide Y., *Decoupling Control of Thrust and Attractive Force of a LIM Using a Space Vector Control Inverter*. IEEE Trans. IA 29(1): 161-167 (1993).

[10] Kotani Y., Morizane T, *The Dynamic Characteristics of LIM Using Disc-Shaped Secondary Side Converted into Linear Motion.* Proc. of ICEM 2012 (2012).

[11] Iwaki K., Morizane T., Kimura N., Taniguchi K., *Characteristics of forces of Linear Induction Motor driven by power source including frequency component synchronous with the motor speed.* Proc. ICEMS 2009, DS1G6-1 (2009).

[12] Morizane T., Tsujikawa K., Kimura N., *The measurement of the dynamic characteristics of LIM with experimental equipment using disc-shaped secondary side*. Proc. of LDIA2011, LIM-II.4 (2011).

[13] Tsuruya K. Morizane T., Kimura N., Omori H., *Disc-Shaped LIM for Attractive and Thrust Force control powered by the source using the Component Synchronous with the Motor Speed.* Proc. of LDIA 2015, CTRL-1.1 (2015).

[14] Tsuruya K. Morizane T., Kimura N., Omori H., *Simultaneous Thrust and Attractive force Control of Linear Induction Motor Driven by Power Source with Frequency Component Synchronous with Motor Speed.* Proc. of EPE'2015 ECCE Europe, DS3f 389 (2015).